

## Anionic clay surface facilitates electron transfer between an excited donor encapsulated within a cationic capsule and a cationic electron acceptor

Natsuki Morita <sup>a</sup>, A. Mohan Raj <sup>b</sup>, Takuya Fujimura <sup>c</sup>, Tetsuya Shimada <sup>a</sup>, Vaidhyanathan Ramamurthy <sup>b,\*</sup>, Shinsuke Takagi <sup>a, \*\*</sup>

<sup>a</sup> Department of Applied Chemistry, Graduate Course of Urban Environmental Sciences, Tokyo Metropolitan University, Minami-ohsawa 1-1, Hachiohji, Tokyo 192-0397, Japan

<sup>b</sup> Department of Chemistry, University of Miami, Coral Gables, Florida 33146-0431, United States

<sup>c</sup> Department of Physics and Materials Science, Interdisciplinary Graduate School of Science and Engineering, Shimane University, 1060 Nishi-kawatsu-cho, Matsue, Shimane 690-8504, Japan



### ARTICLE INFO

#### Keywords:

Supramolecular chemistry  
Cavitands  
Clays  
Electron transfer  
Electrostatic interaction  
Size matching rule

### ABSTRACT

Fluorescence quenching of an excited guest encapsulated within a cationic host by a cationic molecule was examined on an anionic inorganic surface. Repulsion between the host and the quencher was overcome by adsorbing both an anionic surface. Dimethyl stilbene (DMS), octa amine ( $OAm_2^{16+}$ ), viologen derivatives ( $VD^{2+}$ ) and saponite are used as guest, cationic capsule, cationic electron acceptor and anionic inorganic surface, respectively. The fluorescence behavior of DMS within  $OAm_2^{16+}$  (denoted as  $DMS@OAm_2^{16+}$ ) was observed by steady-state and time-resolved fluorescence measurements. As a result of electron transfer the fluorescence of  $DMS@OAm_2^{16+}$  was quenched by  $VD^{2+}$  under the presence of saponite, while no quenching was observed in the absence of saponite. Those results indicate that the dynamic electron transfer between  $DMS@OAm_2^{16+}$  and  $VD^{2+}$  which are electrostatically repulsive, can be observed in the ( $DMS@OAm_2^{16+}$ )- $VD^{2+}$ -saponite triad supramolecular system where the two cationic systems are brought closer by the anionic clay sheet.

### Introduction

Conducting photochemistry in aqueous environment makes the chemistry more sustainable and environmentally friendly. In the context of visible light photocatalysis, organic dyes that absorb in the visible region have attained a prominent position recently. However, most of them are not water-soluble. One of the promising methods to make water-insoluble neutral dyes dissolve in aqueous solution is to complex them with water-soluble hosts such as calixarenes, [1] cyclodextrins [2, 3] and hemicarcerands [4] as containers for neutral dyes. During the last two decades, we have explored the use of organic cavitands such as octa amine ( $OAm^{8+}$ ) and octa acid ( $OAc^{8-}$ ) as containers to solubilize hydrophobic molecules in water. [5-8]  $OAm^{8+}$  and  $OAc^{8-}$  are unusual as hosts as two such molecules assemble to form a capsule that encapsulates one or two guest molecules, probably driven by hydrophobic interactions. Although hosts  $OAm^{8+}$  and  $OAc^{8-}$  are useful to dissolve neutral molecules in aqueous solution (basic or acidic conditions respectively), the charges around them ( $NMe_3^+$  or  $COO^-$ ) would prevent

interaction with molecules of the same charge. For example, interaction between positively charged  $OAm$  capsule and dimethylviologen dication would not be expected.

The electron transfer reactions, which require collision of molecules, have been examined between the excited electron donor encapsulated within  $OAc_2^{16-}$  and the acceptor outside of  $OAc_2^{16-}$  under aqueous condition. [9-12] In the above reactions, anionic  $OAc_2^{16-}$  and cationic acceptor form a weak complex due to the electrostatic attraction that favors ultrafast electron transfer reactions. On the other hand, neutral and anionic molecules work ineffectively for the deactivation of the excited guest within anionic  $OAc_2^{16-}$ . [7] These results prompted us to introduce a reaction field as another approach to achieve efficient electron transfer reactions between guests within capsules and free molecules that do not have attractive interaction between them.

Among various materials, surfaces of clay minerals are known as highly useful chemical reaction field to organize various organic molecules to perform photochemical reactions. [13-15] In particular, it is reported that cationic molecules adsorb on the anionic clay nano-sheets

\* Corresponding author.

\*\* Corresponding author.

E-mail address: [murthy1@miami.edu](mailto:murthy1@miami.edu) (V. Ramamurthy).

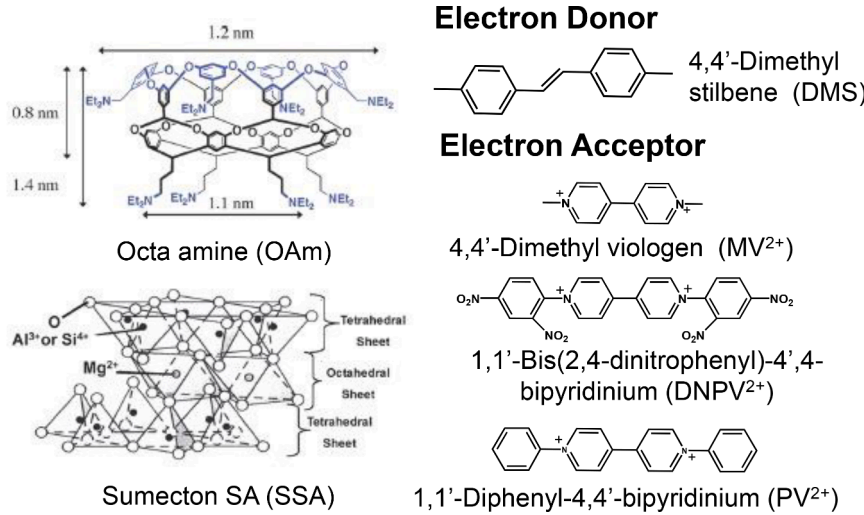


**Fig. 1.** Structure of cavitand (OAm<sup>8+</sup>), neutral electron donor (DMS), clay minerals (SSA) and electron acceptor molecules (MV<sup>2+</sup>, DNPV<sup>2+</sup> and PV<sup>2+</sup>).

densely without aggregation when the distance between anions on the clay and that between cationic molecules compliment each other (size-matching rule). [16–18] By utilizing this molecular condensed field and choosing molecules that obey the size matching rule, efficient intermolecular photochemical reactions have been performed on clay surfaces. [19–24] Recently, we reported that cationic OAm<sup>8+</sup> encapsulating guest can participate in efficient energy transfer reactions on the clay surface. [25–28]

These energy transfer studies motivated us to probe the feasibility of electron transfer between a neutral guest encapsulated in a cationic capsule and a cationic electron acceptor adsorbed on an anionic clay surface. In the absence of clay surface the electron transfer is not expected as the two species would repel each other. However, we visualized that the anionic nanoclay surface would be able to bring them closer and favor electron transfer. To test this possibility, we have used 4,4'-dimethyl stilbene (DMS) and viologen derivatives as neutral electron donor and electron acceptor. The host OAm<sup>8+</sup> is used to solubilize the donor in water through encapsulation and anionic synthetic saponite (Sumecton SA (SSA)) to hold both the cationic capsule and the electron acceptor in proximity (Fig. 1). Their adsorption and photochemical behavior on the saponite surface were examined.

## Experimental section

Sumecton SA (SSA), a typical commercially available synthetic clay, was used as the anionic inorganic nanosheet. SSA was purchased from Kunimine Industries Co., Ltd (Japan). The chemical formula of SSA is  $[(\text{Si}_{7.2} \text{Al}_{0.8})(\text{Mg}_{5.97} \text{Al}_{0.03})\text{O}_{20}(\text{OH})_4]^{0.77} \text{Na}^+$ . The cation exchange capacity (CEC) and surface area of SSA is 99.7 mequiv. g<sup>-1</sup> and 749 m<sup>2</sup> g<sup>-1</sup>, respectively. From these values, the average distance between anions on SSA is calculated to be 1.2 nm assuming an hexagonal array. The organic cavitand with amine functionality (OAm<sup>8+</sup>) was synthesized according to the reported procedure. [6] OAm<sup>8+</sup> is expected to have 8 ammonium groups protonated under acidic conditions. 4,4'-Dimethyl stilbene (DMS) was used as the electron donor. This was solubilized in water by encapsulating it within OAm<sup>16+</sup>. Viologen derivatives (VD<sup>2+</sup>) such as 4,4'-dimethyl viologen (MV<sup>2+</sup>), 1,1'-bis(2,4-dinitrophenyl)-4',4'-bipyridinium (DNPV<sup>2+</sup>) and 1,1'-diphenyl-4,4'-bipyridinium (PV<sup>2+</sup>) were used as electron acceptors [23,29–31]. Based on electrochemical potentials of the donor and acceptor molecules and excited state energy of DMS, electron transfer between excited DMS and viologens are expected to be exothermic. DMS was synthesized by the reported method. [32] 4,4'-Dimethyl viologen dichloride (MV<sup>2+</sup>), 1,1'-bis(2,4-dinitrophenyl)-4',4'-bipyridinium dichloride (DNPV<sup>2+</sup>) and 1,

1'-diphenyl-4,4'-bipyridinium dichloride (PV<sup>2+</sup>) were purchased from Tokyo Chemical Industry Co., Ltd. and used as received.

UV-vis. spectra were recorded on Shimadzu UV-2600 spectrophotometer. Fluorescence spectra were recorded on FS920CDT fluorometer (Edinburgh Analytical Instruments). Time-resolved fluorescence spectra were measured by time-correlated single photon counting using nF920 fluorometer (Edinburgh Analytical Instruments). The samples were excited using LED at 320 nm and the emission decay was monitored at 367 nm. All the measurement was carried out using disposable cells. <sup>1</sup>H NMR spectrum was recorded on Bruker B-500. The intrinsic mass of SSA was determined by thermogravimetric analysis on TG 209 F3 (NETZSCH) or Shimadzu DTG-60H because SSA contains some amount of water at usual temperature and pressure.

The stock solution of DMS@OAm<sub>2</sub><sup>16+</sup> was prepared as follows: 1.23 mg of OAm<sup>8+</sup> was added to 600 μL of water and the solution was sonicated for about 10 minutes. Then 5 μL of 37 % hydrochloride was added to obtain a transparent solution. To this 5 μL of 60 mM DMS in DMSO was added and the solution was shaken well. Further addition of 610 μL of pH1 water gave  $2.46 \times 10^{-4}$  M DMS@OAm<sub>2</sub><sup>16+</sup> in pH1 solution. The encapsulation of DMS within OAm<sub>2</sub><sup>16+</sup> was confirmed by <sup>1</sup>H NMR spectra and the complex formation ratio was turned out to be DMS:OAm<sup>8+</sup> = 1:2. [9] Previously, we had confirmed through NMR titration experiments that DMS forms 1:2 complex with OAm<sup>8+</sup>. The complex where DMS is included within OAm<sub>2</sub><sup>16+</sup> is denoted as DMS@OAm<sub>2</sub><sup>16+</sup>.

The samples for the absorption and photophysical measurements were prepared as follows: SSA dispersed solution was added under stirring to an acidic aqueous solution containing acceptor and the above DMS@OAm<sub>2</sub><sup>16+</sup>. The acidity of the solution was adjusted close to pH1.

## Results and discussion

### Adsorption behavior of DMS@OAm<sub>2</sub><sup>16+</sup> on a clay surface

By mixing the solution of DMS@OAm<sub>2</sub><sup>16+</sup> and SSA in acidic aqueous solution (pH1), the supramolecular complex DMS@OAm<sub>2</sub><sup>16+</sup> adsorbed on the dispersed clay surface was prepared. The supramolecular complex on the surface of SSA is denoted as (DMS@OAm<sub>2</sub><sup>16+</sup>) $\cap$ clay. The typical concentrations are [DMS@OAm<sub>2</sub><sup>16+</sup>] =  $4.1 \times 10^{-7}$  M (40 % vs. CEC) and [SSA] =  $1.6 \times 10^{-2}$  g L<sup>-1</sup>. Under these conditions, clay sheets are exfoliated into a single sheet. In these sheets the minimum distance between cationic site of OAm<sup>8+</sup> is estimated to be 1.1 nm. [25] Thus, OAm<sup>8+</sup> satisfy the size - matching condition for dense adsorption without aggregation on SSA. [16–18] To monitor the adsorption behavior of DMS@OAm<sub>2</sub><sup>16+</sup> on the clay, absorption spectra of the

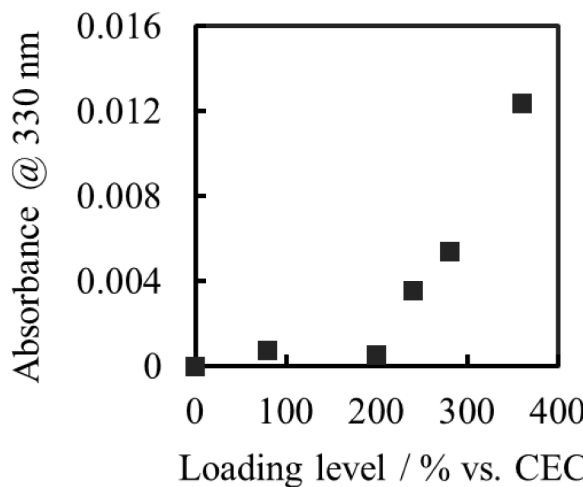


**Fig. 2.** Lambert-Beer plot of filtered solution of DMS@OAm<sub>2</sub><sup>16+</sup>∩clay. [SSA] =  $1.6 \times 10^{-2}$  g/L, [DMS@OAm<sub>2</sub><sup>16+</sup>] =  $0\text{--}3.7 \times 10^{-6}$  M, pH = 1 in aqueous condition. PTFE filter with 0.1  $\mu$ m pores was used.

aqueous solution containing various ratios of the complex and clay were recorded (Fig. S1). Till [DMS@OAm<sub>2</sub><sup>16+</sup>] adsorption reached 800% of CEC of the clay the Beer plot at 323 nm was linear and the spectral shape did not change. This indicates that the absorption spectra of adsorbed and non-adsorbed species are similar suggesting the adsorption behavior cannot be monitored by absorption characteristics of the solution. In addition, fluorescence spectra also did not depend on the loading level of DMS@OAm<sub>2</sub><sup>16+</sup> (Fig. S2). To quantify the adsorbed amount of DMS@OAm<sub>2</sub><sup>16+</sup>, the absorption spectra of the aqueous solution containing various ratios of the DMS@OAm<sub>2</sub><sup>16+</sup> and clay after filtration (PTFE, diameter of the pore size = 0.1  $\mu$ m) were observed (Fig. 2). After filtration, the absorption due to the DMS@OAm<sub>2</sub><sup>16+</sup> was almost negligible below the 200% CEC condition. Above 200% CEC, the absorption showed a linear dependence on the loading. This suggested that the clay nanosheet can adsorb DMS@OAm<sub>2</sub><sup>16+</sup> up to 200% CEC, and above that whatever is added remained in the solution. Based on the fact that a maximum of only 200% adsorption occurred, only 8 cationic sites of the capsule interacted with the clay surface. Thus, the surface distribution of adsorbed DMS@OAm<sub>2</sub><sup>16+</sup> on SSA is as shown in Figure S3.

#### Adsorption behavior of DMS@OAm<sub>2</sub><sup>16+</sup>-VD<sup>2+</sup> on the clay surface

Absorption spectra of VD<sup>2+</sup>∩clay, DMS@OAm<sub>2</sub><sup>16+</sup>∩clay, (DMS@OAm<sub>2</sub><sup>16+</sup>-VD<sup>2+</sup>)∩clay and sum of absorption spectra of VD<sup>2+</sup>∩clay and DMS@OAm<sub>2</sub><sup>16+</sup>∩clay are shown in Fig. 3. Viologen derivatives MV<sup>2+</sup>, DNPV<sup>2+</sup> and PV<sup>2+</sup> were used as electron acceptors. The absorption spectra of DMS@OAm<sub>2</sub><sup>16+</sup>-VD<sup>2+</sup>)∩clay overlap with sum of those of VD<sup>2+</sup>∩clay and DMS@OAm<sub>2</sub><sup>16+</sup>∩clay. This confirms the absence of specific interaction between DMS@OAm<sub>2</sub><sup>16+</sup> and VD<sup>2+</sup>s on clay.

#### Photochemical behavior of DMS@OAm<sub>2</sub><sup>16+</sup>-VD<sup>2+</sup> on the clay surface

To investigate the electron transfer between DMS@OAm<sub>2</sub><sup>16+</sup> and VD<sup>2+</sup>s on the clay surface, steady-state fluorescence spectra of DMS@OAm<sub>2</sub><sup>16+</sup>∩clay with and without VD<sup>2+</sup>s were recorded (Fig. 4). The fluorescence intensity of DMS@OAm<sub>2</sub><sup>16+</sup> was not affected by the addition of MV<sup>2+</sup>. On the other hand, the fluorescence intensity of DMS@OAm<sub>2</sub><sup>16+</sup> at 369 nm decreased by 49% and 41% by the addition of DNPV<sup>2+</sup> and PV<sup>2+</sup>, respectively. In the case of PV<sup>2+</sup>, the emission due to the direct excitation of PV<sup>2+</sup> was superimposed. While the quenching was not observed for MV<sup>2+</sup>, moderate quenching was observed for (DMS@OAm<sub>2</sub><sup>16+</sup>-DNPV<sup>2+</sup>)∩clay and (DMS@OAm<sub>2</sub><sup>16+</sup>-PV<sup>2+</sup>)∩clay systems. Control experiments established that the absence of fluorescence quenching of DMS@OAm<sub>2</sub><sup>16+</sup> by VD<sup>2+</sup>s in solution without SSA (Fig. S4).

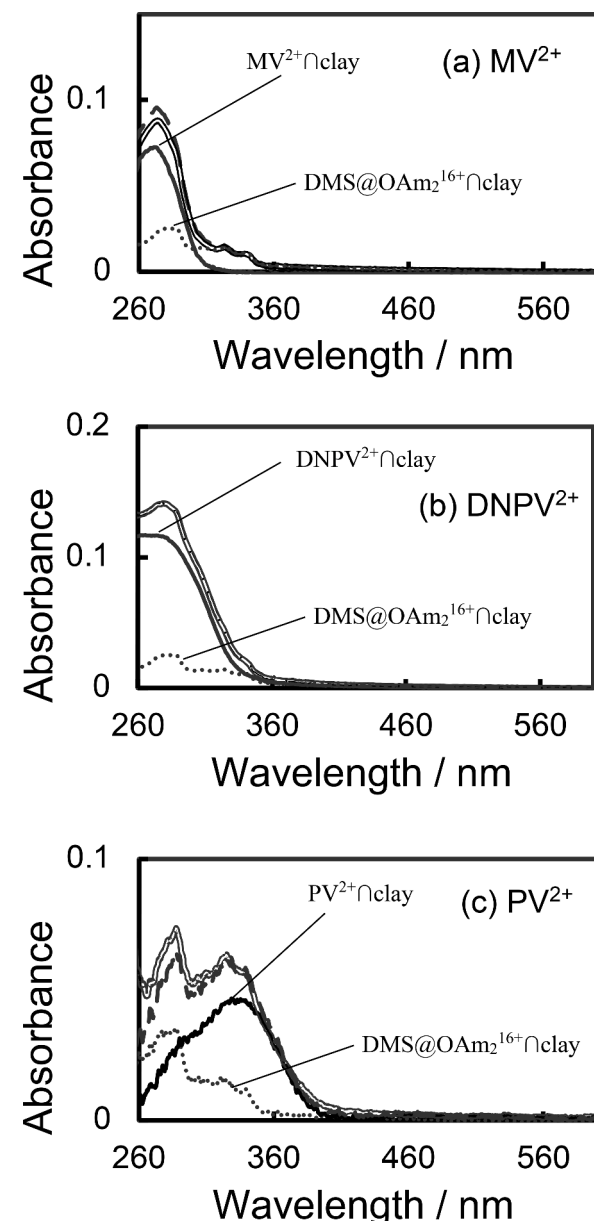


**Fig. 3.** Absorption spectra of VD<sup>2+</sup>∩clay, DMS@OAm<sub>2</sub><sup>16+</sup>∩clay, (DMS@OAm<sub>2</sub><sup>16+</sup>-VD<sup>2+</sup>)∩clay and sum of absorption spectra of VD<sup>2+</sup>∩clay and DMS@OAm<sub>2</sub><sup>16+</sup>∩clay. VD<sup>2+</sup>s are MV<sup>2+</sup> (a), DNPV<sup>2+</sup> (b) and PV<sup>2+</sup> (c). Continuous line: VD<sup>2+</sup>∩clay, Dotted line: DMS@OAm<sub>2</sub><sup>16+</sup>∩clay, Double line: (DMS@OAm<sub>2</sub><sup>16+</sup>-VD<sup>2+</sup>)∩clay, Broken line: Sum of absorption spectra of VD<sup>2+</sup>∩clay and DMS@OAm<sub>2</sub><sup>16+</sup>∩clay. [DMS@OAm<sub>2</sub><sup>16+</sup>] =  $4.1 \times 10^{-7}$  M (40% vs. CEC), [MV<sup>2+</sup>] = [DNPV<sup>2+</sup>] =  $2.4 \times 10^{-6}$  M (30% vs. CEC), [PV<sup>2+</sup>] =  $1.6 \times 10^{-6}$  M (20% vs. CEC), [Clay] =  $1.6 \times 10^{-2}$  g L<sup>-1</sup>, pH = 1 in aqueous condition.

This confirmed the critical role SSA played in the electron transfer process. Apparently, the SSA surface is essential to bring the cationic capsule and the cationic electron acceptors closer.

To probe the mechanism of the steady-state fluorescence quenching, time-resolved fluorescence measurements were carried out. The fluorescence decay curves of DMS@OAm<sub>2</sub><sup>16+</sup> with and without VD<sup>2+</sup>s on SSA are shown in Fig. 5. The excited lifetime of DMS@OAm<sub>2</sub><sup>16+</sup> on clay ( $\tau = 1.3$  ns) was not affected by the addition of MV<sup>2+</sup>. Absence of lifetime change and fluorescence quenching in presence of MV<sup>2+</sup> suggest that MV<sup>2+</sup> does not accept electron from encapsulated excited DMS. On the other hand, an apparent lifetime quenching was observed for (DMS@OAm<sub>2</sub><sup>16+</sup>-DNPV<sup>2+</sup>)∩clay (Fig. 5). The decay curve can be fitted as two components ( $\tau_1 = 0.7$  ns (58%) and  $\tau_2 = 1.3$  ns (42%)). The

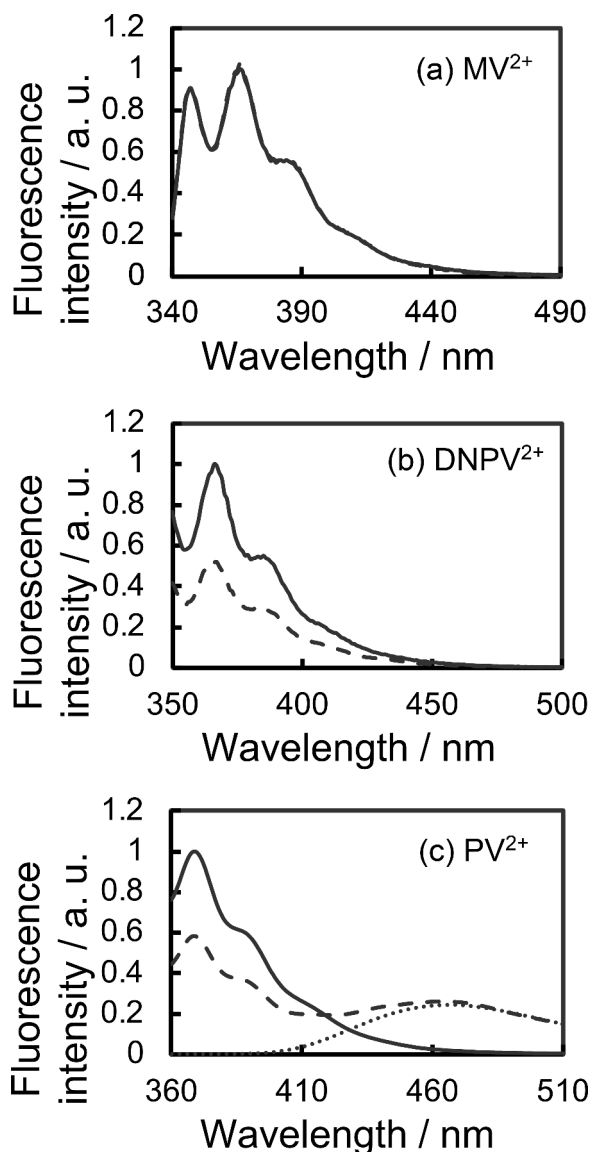


**Fig. 4.** Steady-state fluorescence spectra of  $\text{DMS}@\text{OAm}_2^{16+}\cap\text{clay}$  with and without  $\text{VD}^{2+}$ . Continuous line:  $\text{DMS}@\text{OAm}_2^{16+}\cap\text{clay}$ , Broken line:  $(\text{DMS}@\text{OAm}_2^{16+}\cap\text{VD}^{2+})\cap\text{clay}$ , Dotted line (only for (c)):  $\text{PV}^{2+}\cap\text{clay}$ .  $[\text{DMS}@\text{OAm}_2^{16+}] = 4.1 \times 10^{-7} \text{ M}$  (40 % vs. CEC),  $[\text{MV}^{2+}] = [\text{DNPV}^{2+}] = 2.4 \times 10^{-6} \text{ M}$  (30 % vs. CEC),  $[\text{PV}^{2+}] = 1.6 \times 10^{-6} \text{ M}$  (20 % vs. CEC),  $[\text{Clay}] = 1.6 \times 10^{-2} \text{ g L}^{-1}$ ,  $\text{pH}=1$  in aqueous condition, Excitation wavelength: 335 nm for  $\text{MV}^{2+}$  and 345 nm for  $\text{PV}^{2+}$ ,  $\text{DNPV}^{2+}$ .

decrease in lifetime indicate that the quenching process observed for  $(\text{DMS}@\text{OAm}_2^{16+}\cap\text{DNPV}^{2+})\cap\text{clay}$  involves a dynamic component.

An important question that needs to be addressed relates to the difference in quenching behavior between  $\text{MV}^{2+}$  and  $\text{DNPV}^{2+}$ . Based on their redox potentials in aqueous condition, the  $\Delta G$  for electron transfer from excited DMS to  $\text{MV}^{2+}$  and  $\text{DNPV}^{2+}$  are exothermic by -1.3 eV and -1.8 eV, respectively. In spite of this, electron transfer reaction was observed only for  $\text{DNPV}^{2+}$ . There are several possibilities: (a) The reorganization energy ( $\lambda$ ) for electron transfer in the two systems may not be similar. (b) The reduction potentials for the two systems on the clay surface may not be the same as in solution. At this stage with limited experiments, we are unable to identify the origin of the above difference. Further work is planned.

In conclusion, we have established the need for anionic clay surface as a reaction field to bring about electron transfer between electrically repulsive  $\text{DMS}@\text{OAm}_2^{16+}$  donor and  $\text{DNPV}^{2+}$  acceptor. The role of clay

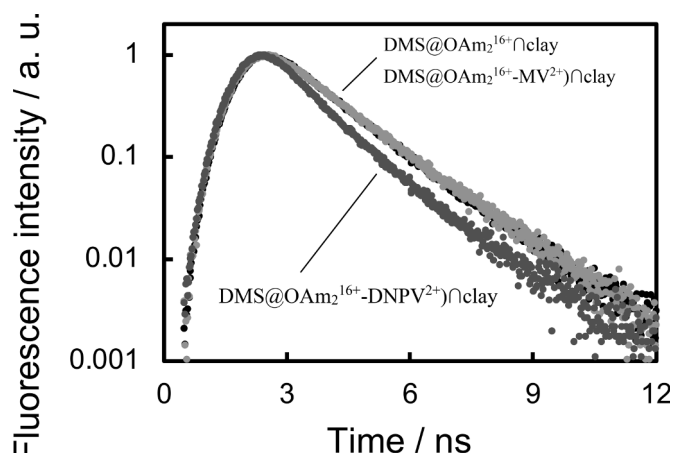


**Fig. 5.** Fluorescence decay curves of  $\text{DMS}@\text{OAm}_2^{16+}$  with and without  $\text{VD}^{2+}$ s. Black line:  $\text{DMS}@\text{OAm}_2^{16+}\cap\text{clay}$ , Gray line:  $(\text{DMS}@\text{OAm}_2^{16+}\cap\text{MV}^{2+})\cap\text{clay}$ , Dark gray line:  $(\text{DMS}@\text{OAm}_2^{16+}\cap\text{DNPV}^{2+})\cap\text{clay}$ .  $[\text{DMS}@\text{OAm}_2^{16+}] = 4.1 \times 10^{-7} \text{ M}$  (40 % vs. CEC),  $[\text{MV}^{2+}] = [\text{DNPV}^{2+}] = 2.4 \times 10^{-6} \text{ M}$  (30 % vs. CEC),  $[\text{Clay}] = 1.6 \times 10^{-2} \text{ g L}^{-1}$ ,  $\text{pH}=1$  in aqueous condition.

surface in this process can be visualized follows: (a) Anionic clay surface concentrates the cationic donor and acceptor specie. (b) Such localization facilitates quenching of excited  $\text{DMS}@\text{OAm}_2^{16+}$  even at low concentrations of  $\text{DNPV}^{2+}$ . (c) Electrostatic repulsion between  $\text{DMS}@\text{OAm}_2^{16+}$  and  $\text{DNPV}^{2+}$  is practically suppressed, because of the strong electrostatic interactions between anionic clay surface and guest ( $\text{DNPV}^{2+}$  and  $\text{DMS}@\text{OAm}_2^{16+}$ ) caused by 'size-matching condition'. This study has brought out the value of a trimolecular supramolecular assembly consisting of a synthetic organic capsule, inorganic clay nanosheet and a regular organic molecule in bringing out a phenomenon that can't happen in the absence of any one of the three in water.

#### Declaration of Competing Interest

The authors declare that they have no known competing financial interests or personal relationships that could have appeared to influence the work reported in this paper.

#### Data availability

Data will be made available on request.

#### Acknowledgements

In ST's laboratory this work has been partly supported by a Grant-in-Aid for Scientific Research (B) (No. 24350100) and a Grant-in-Aid for Scientific Research on Innovative Areas "All Nippon Artificial Photosynthesis Project for Living Earth" (AnApple, No. 25107521). VR thanks the National Science Foundation (CHE- 2204046) for financial support. The authors dedicate this contribution to our dear colleague, friend and leader in the field of photoinduced electron transfer Professor Emeritus Kazuhiko Mizuno on the occasion of his 75th birthday.

#### Supplementary materials

Supplementary material associated with this article can be found, in the online version, at [doi:10.1016/j.jpp.2023.100204](https://doi.org/10.1016/j.jpp.2023.100204).

#### References

- [1] R. Kaliappan, V. Ramamurthy, *J. Photochem. Photobiol. A - Chem.* 207 (2009) 32–37.
- [2] V. Ramamurthy, D.F. Eaton, *Acc. Chem. Res.* 21 (1988) 300–306.

[3] N. Vallavouj, J. Sivaguru, *Chem. Soc. Rev.* 43 (2014) 4084–4101.

[4] K.I. Jankowska, C.V. Pagba, E.L. Piatnitsk Chekler, K. Deshayes, P. Piotrowiak, *J. Am. Chem. Soc.* 132 (2010) 16423–16431.

[5] V. Ramamurthy, *Acc. Chem. Res.* 48 (2015) 2904–2917.

[6] R. Kulasekharan, V. Ramamurthy, *Org. Lett.* 13 (2011) 5092–5095.

[7] M. Porel, S. Jockusch, M.F. Ottaviani, N.J. Turro, V. Ramamurthy, *Langmuir* 27 (2011) 10548–10555.

[8] S. Gupta, A. Adhikari, A.K. Mandal, K. Bhattacharyya, V. Ramamurthy, *J. Phys. Chem. C* 115 (2011) 9593–9600.

[9] M. Porel, S. Jockusch, A. Parthasarathy, V.J. Rao, N.J. Turro, V. Ramamurthy, *Chem. Commun.* 48 (2012) 2710–2712.

[10] M. Porel, C. Chuang, C. Burda, V. Ramamurthy, *J. Am. Chem. Soc.* 134 (2012) 14718–14721.

[11] M. Porel, A. Klimczak, M. Freitag, E. Galoppini, V. Ramamurthy, *Langmuir* 28 (2012) 3355–3359.

[12] P. Piotrowiak, *Chem. Soc. Rev.* 28 (1999) 143–150.

[13] T. Shichi, K. Takagi, *J. Photochem. Photobio. C – Photochem. Rev.* 1 (2000) 113–130.

[14] J. Bujdák, *App. Clay Sci.* 34 (2006) 58–73.

[15] S. Belusakova, K. Lang, J. Bujdák, *J. Phys. Chem. C* 119 (2015) 21784–21794.

[16] S. Takagi, T. Shimada, M. Eguchi, T. Yui, H. Yoshida, D.A. Tryk, H. Inoue, *Langmuir* 18 (2002) 2265–2272.

[17] T. Egawa, H. Watanabe, T. Fujimura, Y. Ishida, M. Yamato, D. Masui, T. Shimada, H. Tachibana, H. Yoshida, H. Inoue, S. Takagi, *Langmuir* 27 (2011) 10722–10729.

[18] S. Takagi, T. Shimada, Y. Ishida, T. Fujimura, D. Masui, H. Tachibana, M. Eguchi, H. Inoue, *Langmuir* 29 (2013) 2108–2119.

[19] S. Takagi, M. Eguchi, H. Inoue, *Res. Chem. Intermed.* 33 (2007) 177–189.

[20] Y. Ishida, T. Shimada, D. Masui, H. Tachibana, H. Inoue, S. Takagi, *J. Am. Chem. Soc.* 133 (2011) 14280–14286.

[21] Y. Ishida, D. Masui, H. Tachibana, H. Inoue, T. Shimada, S. Takagi, *Appl. Mater. Interfaces* 4 (2012) 811–816.

[22] Y. Ohtani, T. Shimada, S. Takagi, *J. Phys. Chem. C* 119 (2015) 18896–18902.

[23] S. Konno, T. Fujimura, Y. Ohtani, T. Shimada, H. Inoue, S. Takagi, *J. Phys. Chem. C* 118 (2014) 20504–20510.

[24] Y. Ishida, T. Shimada, H. Tachibana, H. Inoue, S. Takagi, *J. Phys. Chem. A* 116 (2012) 12065–12072.

[25] Y. Ishida, R. Kulasekharan, T. Shimada, S. Takagi, V. Ramamurthy, *Langmuir* 29 (2013) 1748–1753.

[26] Y. Ishida, R. Kulasekharan, T. Shimada, S. Takagi, V. Ramamurthy, *J. Phys. Chem. C* 118 (2014) 10198–10203.

[27] T. Fujimura, E. Ramasamy, Y. Ishida, T. Shimada, S. Takagi, V. Ramamurthy, *Phys. Chem. Chem. Phys.* 18 (2016) 5404–5411.

[28] T. Tsukamoto, E. Ramasamy, T. Shimada, S. Takagi, V. Ramamurthy, *Langmuir*, 32 (2016) 2920–2927.

[29] C.L. Bird, A.T. Kuhn, *Chem. Soc. Rev.* 10 (1981) 49–82.

[30] J.C. Russel, D.G. Whitten, A.M. Braun, *J. Am. Chem. Soc.* 103 (1981) 3219–3220.

[31] L. Chen, D.W. McBranch, H. Wang, R. Helgeson, F. Wudl, D.G. Whitten, *Proc. Natl. Acad. Sci.* 96 (1999) 12287–12292.

[32] A. Parthasarathy, V. Ramamurthy, *Photochem. Photobiol. Sci.* 10 (2011) 1455–1462.